12-1-2016

Efficacy of the Biomaterials 3 wt%-nanostrontium-hydroxyapatite-enhanced Calcium Phosphate Cement (nanoSr-CPC) and nanoSr-CPC-incorporated Simvastatin-loaded Poly(lactic-co-glycolic-acid) Microspheres in Osteogenesis Improvement

Reza Masaeli
Tehran University of Medical Sciences

Tahereh S. Jafarzadeh Kashi
Tehran University of Medical Sciences

Rassoul Dinarvand
Tehran University of Medical Sciences

Vahid Rakhshan
Tehran University of Medical Sciences

Hossein Shahoon
Shahed University

See next page for additional authors

Authors
Reza Masaeli, Tahereh S. Jafarzadeh Kashi, Rassoul Dinarvand, Vahid Rakhshan, Hossein Shahoon, Behzad Hooshmand, Fatemeh Mashhadi Abbas, Majid Raz, Alireza Rajabnejad, Hossein Eslami, Kimia Khoshroo, Mohammadreza Tahriri, and Lobat Tayebi

Efficacy of The Biomaterials 3 wt%-Nanostrontium-Hydroxyapatite-Enhanced Calcium Phosphate Cement (nanosr-CPC) And nanosr-CPC-Incorporated Simvastatin-Loaded Poly(Lactic-Co-Glycolic-Acid) Microspheres in Osteogenesis Improvement: An Explorative Multi-Phase Experimental in Vitro/Vivo Study

Reza Masaeli
Dental Biomaterials Department, School of Dentistry,
Tehran University of Medical Sciences,
Tehran, Iran
Tehereh Sadat Jafarzadeh Kashi
Dental Biomaterials Department, School of Dentistry,
Tehran University of Medical Sciences,

Materials Science and Engineering: C, Vol 69 (December 1, 2016): pg. 780-788. DOI.

Tehran, Iran
Iranian Tissue Bank and Research Center,
Tehran University of Medical Sciences,
Tehran, Iran

Rassoul Dinarvand

Department of Pharmaceutics, Faculty of Pharmacy,
Tehran University of Medical Sciences,
Tehran, Iran

Vahid Rakhshan

Iranian Tissue Bank and Research Center,
Tehran University of Medical Sciences,
Tehran, Iran

Hossein Shahoon

Department of Oral and Maxillofacial Surgery,
School of Dentistry, Shahed University,
Tehran, Iran

Behzad Hooshmand

Department of Periodontology, School of Dentistry,
Shahid Beheshti University of Medical Sciences,
Tehran, Iran

Fatemeh Mashhadi Abbas

Department of Oral and Maxillofacial Pathology,
School of Dentistry, Shahid Beheshti Medical Science University,
Tehran, Iran

Majid Raz

Biomaterials Group, Faculty of Biomedical Engineering,
Amirkabir University of Technology,
Tehran, Iran

Alireza Rajabnejad

Biomaterials Group, Faculty of Biomedical Engineering,
Amirkabir University of Technology,
Tehran, Iran

Materials Science and Engineering: C, Vol 69 (December 1, 2016): pg. 780-788. DOI.

Hossein Eslami

Biomaterials Group, Faculty of Biomedical Engineering,
Amirkabir University of Technology,
Tehran, Iran

Kimia Khoshroo

Dental Biomaterials Department, School of Dentistry,
Tehran University of Medical Sciences,
Tehran, Iran
Department of Developmental Sciences, School of Dentistry,
Marquette University,
Milwaukee, WI,

Mohammadreza Tahriri

Dental Biomaterials Department, School of Dentistry,
Tehran University of Medical Sciences,
Tehran, Iran
Iranian Tissue Bank and Research Center,
Tehran University of Medical Sciences,
Tehran, Iran
Biomaterials Group, Faculty of Biomedical Engineering,
Amirkabir University of Technology,
Tehran, Iran
Department of Developmental Sciences, School of Dentistry,
Marquette University,
Milwaukee, WI,

Lobat Tayebi

Iranian Tissue Bank and Research Center,
Tehran University of Medical Sciences,
Tehran, Iran
Biomaterials and Advanced Drug Delivery Laboratory,
School of Medicine,
Stanford University, Palo Alto

Materials Science and Engineering: C, Vol 69 (December 1, 2016): pg. 780-788. DOI.

Abstract

Aims: The purpose of this multi-phase explorative in vivo animal/surgical and in vitro multi-test experimental study was to (1) create a 3 wt%-nanostrontium hydroxyapatite-enhanced calcium phosphate cement (Sr-HA/CPC) for increasing bone formation and (2) creating a simvastatin-loaded poly(lactic-*co*-glycolic acid) (SIM-loaded PLGA) microspheres plus CPC composite (SIM-loaded PLGA + nanostrontium-CPC). The third goal was the extensive assessment of multiple in vitro and in vivo characteristics of the above experimental explorative products in vitro and in vivo (animal and surgical studies).

Methods and results pertaining to Sr-HA/CPC: Physical and chemical properties of the prepared Sr-HA/CPC were evaluated. MTT assay and alkaline phosphatase activities, and radiological and histological examinations of Sr-HA/CPC, CPC and negative control were compared. X-ray diffraction (XRD) indicated that crystallinity of the prepared cement increased by increasing the powder-to-liquid ratio. Incorporation of Sr-HA into CPC increased MTT assay (biocompatibility) and ALP activity ($P < 0.05$). Histomorphometry showed greater bone formation after 4 weeks, after implantation of Sr-HA/CPC in 10 rats compared to implantations of CPC or empty defects in the same rats ($n = 30$, ANOVA $P < 0.05$).

Methods and results pertaining to SIM-loaded PLGA microspheres + nanostrontium-CPC composite: After SEM assessment, the produced composite of microspheres and enhanced CPC were implanted for 8 weeks in 10 rabbits, along with positive and negative controls, enhanced CPC, and enhanced CPC plus SIM ($n = 50$). In the control group, only a small amount of bone had been regenerated (localized at the boundary of the defect); whereas, other groups showed new bone formation within and around the materials. A significant difference was found in the osteogenesis induced by the groups sham control (16.96 ± 1.01), bone materials (32.28 ± 4.03), nanostrontium-CPC (24.84 ± 2.6), nanostrontium-CPC-simvastatin (40.12 ± 3.29), and SIM-loaded PLGA + nanostrontium-CPC (44.8 ± 6.45) (ANOVA $P < 0.001$). All the pairwise comparisons were significant (Tukey $P < 0.01$), except that of nanostrontium-CPC-simvastatin and SIM-loaded PLGA + nanostrontium-CPC. This confirmed the efficacy of the SIM-loaded PLGA + nanostrontium-CPC composite, and its superiority over all materials except SIM-containing nanostrontium-CPC.

Keywords: Biomaterials, Drug delivery systems, Calcium phosphate cement (CPC), Strontium, Hydroxyapatite, Brushite, Bone formation, Simvastatin, Poly(lactic-*co*-glycolic acid) microspheres

1. Introduction

In 1980s, calcium phosphate cements (CPCs) were discovered by LeGeros and Chow et al.[1] Calcium phosphate cements are used as the bone substitute materials and can serve as injectable pastes to fill defects, while being biocompatible and osteoconductive.[2,3] A bioactive material is one that can bind with the surrounding bone without the

formation of fibrous tissue.[4] Bioactivity, together with the perfect adaptability of the cement paste leads to a stable connection between defect and implant and boost bone healing process.[5,6] The main reaction of calcium phosphate cements is the cementing action of acidic and basic calcium phosphate compounds in an aqueous solution.[1,2,7] Calcium phosphate cements are formed by a chemical reaction between two phases: the dry powder phase which is a combination of calcium orthophosphate, and the liquid phase which is water or a calcium or phosphate-containing aqueous solution.[1,2,4,7,8] After mixing the powder phase with the liquid phase, a paste forms that sets and hardens into a solid mass. One of the advantages of calcium phosphate cements is that no heat is generated during cementation reaction and the cementation process is not exothermic (thus, no risk of hyperthermia).[2,3,7,9,10] Furthermore calcium phosphate cements are intrinsically microporous, as a result of extra aqueous solution leaving the material after hardening. This property can be used for carrying of biological fluids into CPCs and causes degradation and replacement of CPCs by bone. Degradation rate depends on the composition and microstructure of the cement. Degradation products are well absorbed by the surrounding tissues.[11,12,13,14]

Despite having many advantages, calcium phosphate cements have some drawbacks including poor mechanical properties. Like most ceramics, they are brittle. Furthermore, due to their intrinsic porous structure, their strength is lower than acrylic cements. This drawback has limited their application.[11,15,16,17]

There are two main calcium phosphate cements: hydroxyapatite and dicalcium phosphate dehydrate (brushite). The final product formed by the liquid and solid phase depends on pH of the solution. Hydroxyapatite forms in pHs higher than 4.2 while brushite (DCPD) forms when the pH is lower than 4.2. Solubility of brushite is greater than hydroxyapatite at physiological pH. In fact brushite is metastable under physiological conditions and can be resorbed more quickly than hydroxyapatite.[2,8,18]

Brushite cements have generally short setting times (about 30 to 60 s) that limit their use as orthopedic applications. To make these cements suitable for orthopedic usage, specific setting retardants (such as pyrophosphate ions or citrates) are usually added to slow

down the setting process by inhibiting nucleation and growth of calcium phosphate crystals.[7,16,19,20] Moreover, some ions like Sr, Zn, and Mg can serve as enzyme cofactors in bone regeneration process.[21,22,23] Thus, the incorporation of these ions in biomaterials can improve bone tissue healing.[24,25]

Strontium can stimulate osteoblast differentiation and inhibit osteoclast activity and therefore is a valuable ion in treatment of osteoporosis. Hence, there are interests in incorporating strontium in calcium phosphate cements. Incorporation of strontium affects the reactivity of the cement but can also modify the final composition of the material.[24,25,26]

A recent advent in pharmacology is solid polymer biodegradable particulates such as micro and sub-micron spheres with high dissolution rates, which might be of use in locally targeted pharmaceutical delivery and regeneration of injured tissues.[27,28,29] Because of their biodegradation potential and physiological removal, poly(lactic-*co*-glycolic acid) (PLGA) microspheres might be a proper candidate for such drug delivery systems.[28,30,31] Simvastatin (SIM) is a hypolipidemic drug capable of inducing bone regeneration; hence it might be loaded into PLGA microspheres to possibly improve stability of microspheres after formation while also improving the bone regeneration.[28,32,33]

In this study, the structural, physicochemical and biological properties of the type of calcium phosphate cements modified by strontium ion were evaluated. Also its effect on bone generation was examined. Afterwards, a new form of SIM-PLGA was created by the addition of nanostrontium-enhanced CPC. Its efficacy in improving osteogenesis was assessed.

2. Materials and methods

2.1. Overview

In the first phase of this study (in vitro), an optimum ratio of power to liquid (P/L) was selected (among three available ratios) for producing 3 wt% nanostrontium-enhanced CPC with the best in vitro

Materials Science and Engineering: C, Vol 69 (December 1, 2016): pg. 780-788. DOI.

properties. The recommended ratio was then used in next phases: in the second phase, the 3 wt% nanostrontium-enhanced CPC was assessed with various in vitro biological tests and then was compared against CPC as well as negative controls in rat. In the third phase (in vitro), the nanostrontium-enhanced CPC was composited with simvastatin-loaded poly(lactic-*co*-glycolic acid) (SIM-loaded PLGA) microspheres. In the last phase the properties of this "SIM-loaded PLGA + 3 wt% nanostrontium-enhanced CPC" composite biomaterial was evaluated in vitro. Then efficacy of this composite material in ontogenesis induction was evaluated in vivo (rabbit) against the materials: 3 wt% nanostrontium-enhanced CPC and 3 wt% nanostrontium-enhanced CPC plus simvastatin, a negative control (sockets left empty after bone trephining) as well as a positive control (experimental bone defects filled with the animal's trephined bone transplanted from the negative control sites). This study was conducted in accordance with the regulations and approval of the Institutional Animal Care and Ethical Committee of the Tehran University of Medical Sciences.

2.2. Preparation of nanostrontium-enhanced CPC

To prepare calcium phosphate cement powder in this research, one gram of tetracalcium phosphate ($Ca_4P_2O_9$, TTCP) with a controlled mean particle size of 10 μm was synthesized following the method from the reaction of dicalcium phosphate dihydrate ($CaHPO_4{\cdot}2H_2O$, DCPD; Merck Co. Kenilworth, New Jersey, United States) and calcium carbonate ($CaCO_3$). Afterwards, disodium hydrogen phosphate (Na_2HPO_4; Merck) was added to the mixture; three different amounts of Na_2HPO_4 were added, in order to create 3 different powder-to-liquid ratios 1.205 ml (P/L = 0.83), 0.8 ml (P/L = 1.25), and 0.645 ml (P/L = 1.55). Finally, 3 wt% of synthesized nanostrontium-substituted hydroxyapatite (Sr-HA) (10% of calcium in hydroxyapatite was replaced with strontium) was added to the prepared cement. The calcium phosphate cement powder was mechanically ground to the mean particle size distribution of 3 mm; then it was vacuum-packed and g-ray-sterilized (20 kGy). The size of nanoparticles is evident in Fig. 1.

Materials Science and Engineering: C, Vol 69 (December 1, 2016): pg. 780-788. DOI.

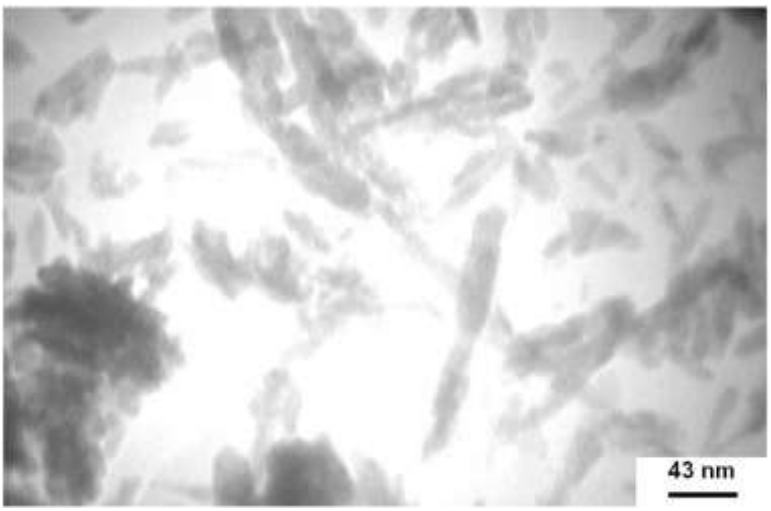

Fig. 1. Transmission electron micrograph of the synthetized nanostrontium hydroxyapatite.

2.3. Characterization of nanostrontium-enhanced CPC

2.3.1. X-ray diffraction analysis

XRD patterns of the prepared calcium phosphate cements (CPCs) were obtained at room temperature using a very high-resolution Cu-K_α radiation diffraction system (Equinox3000, INEL, Artenay, France) operating at a voltage of 40 kV and a current of 30 mA. CPCs were analyzed in the 2θ angle range of 0–80°, and their patterns were studied to determine the crystal phases present in the samples.

2.3.2. Fourier transform infrared spectroscopy (FTIR) analysis

Infrared spectroscopy was carried out to determine the chemical composition of the prepared microspheres using FTIR (Nicolet, USA) operating in the wavenumber range of 400–4000 cm^{-1} at the absorption mode.

2.3.3. Simultaneous thermal analysis

Simultaneous thermal analysis (STA) generally refers to the simultaneous application of thermogravimetry (TGA) and differential scanning calorimetry (DSC) to one and the same sample in a single instrument. A thermoanalyzer (STA; Polymer Laboratories PL-STA

1640) that was heated from room temperature up to ~ 1000 °C with the warming rate of 10 °C/min was used to record the conventional thermoanalytical curves.

2.3.4. Scanning electron microscopy (SEM)

The prepared microspheres were coated with a thin layer of gold by sputtering (Emitech K450X, England). The microstructure of the cement samples was observed using a scanning electron microscope (AIS-2100 780, Seron, South Korea) that operated at an acceleration voltage of 20 kV.

2.3.5. Setting time measurement

The powders of TTCP/DCPD were mixed with ratios of 1:1; and then were mixed with liquid phase for a minute at room temperature. Cement mixture was poured in a plastic mold to set. Setting time of the prepared cement was measured using Vicat test according to the ASTM-C-18798 standard.

2.3.6. Mechanical properties

In accordance with the ISO 14544, the modulus of the cements was measured using a mechanical testing machine (SMT-20, Santam). Cylindrical samples with length-to-diameter ratio of 2:1 (10 mm in length and 5 mm in diameter) were prepared. The load was applied at the cross-head speed of 1 mm/min until the specimen was compressed to approximately 30% of its original length. The elastic modulus was determined as the slope of the initial linear portion of the stress–strain curve.

2.3.7. Inductively coupled plasma (ICP) analysis

The interactions between the cements and a biological medium were carried out at 37 °C for 10, 20, and 110 days by immersing about 10 mg of cement in a simulated body fluid, the composition of which is almost identical to that of human plasma. These in vitro assays were conducted under static conditions: biological fluids were not renewed and therefore contained only limited amounts of P and Ca. Inductively coupled plasma atomic emission spectroscopy (ICP-

AES; Agilent, USA) was used to analyze the biological fluid before and after cement interactions.

2.3.8. Biological evaluation

2.3.8.1. In vitro study

2.3.8.1.1. MTT assay

For measuring the cell viability of the prepared samples MTT (3-(4, 5dimethylthiazol-2-yl)-2, 5-diphenyltetrazolium bromide) assay was used. At first, under standard culturing conditions SAOS-2 cells were seeded on 96 well plates at a density of 1×10^4 cells per well. The cells were incubated on the samples for 3 and 7 days. After the incubation, the medium was removed and a medium containing 10% of MTT solution was added. Then, the plates were incubated at 37 °C for 4 h. The medium was then removed and 100 μl of solubilization buffer (Triton-X 100, 0.1 N HCl and isopropanol) were added to each well to dissolve the formazan crystals, which have been produced due to the activity of living cells in MTT solution. The absorbance of the lysate was measured in a microplate reader at a wavelength of 570 nm.

2.3.8.1.2. Alkaline phosphatase activity

Alkaline phosphatase (ALP) is an enzyme whose production signifies proliferation and differentiation of osteoblasts. An ALP assay kit was used to measure ALP activity according to the manufacturer's protocol (Biocat, Heidelberg, Germany). Briefly, human osteosarcoma cell lines (SAOS-2) were seeded in 24-well cell culture plates at a density of 1×10^4 cells/cm^2. The glass samples (n = 5) were placed in the wells. Three wells in the absence of glass samples were used as negative controls. The plates were incubated for 3 and 7 days at 37 °C in humidified air with 5% CO_2 with half media. Then, the supernatant of each well was removed and the cell layer was rinsed twice with PBS, homogenized with 1 ml Tris buffer, and sonicated for 4 min on ice. Aliquots of 20 ml were incubated with 1 ml of a *p*-nitrophenyl phosphate solution at 30 °C for up to 5 min. Cellular alkaline phosphatase activity was determined by the conversion of *p*-nitrophenyl phosphate to *p*-nitrophenol. It was monitored by following

the absorption at 405 nm. It was converted to enzyme activity using the *p*-nitrophenol standard absorption curve.

2.3.8.2. In vivo study

From the above in vitro experiments, the optimum powder-to-liquid ratio for 3 wt% nanostrontium-enhanced CPC was determined as 0.83 which could provide the best setting time, and hence proper for surgical procedures. This ratio was used for all the in vivo experiments mentioned below, as well as for producing the composite of nanostrontium-enhanced CPC with simvastatin-loaded poly(lactic-*co*-glycolic acid) microspheres.

2.3.8.2.1. Animals, surgical procedures, and experimental grouping

The goal of this part was to comparatively evaluate the efficacy of the produced material in bone morphogenesis. Ten 10-week-old male Sprague–Dawley rats with an initial weight of 250–290 g were purchased from the Pasteur Institute for the in vivo study. Animals were anesthetized by means of intramuscular injection using ketamine (80 mg/kg) and xylazine (10 mg/kg). A full-thickness incision was made in the anterior region of the calvarium and a 5-mm diameter full-thickness bone defect was prepared using a trephine drill under continuous sterile saline irrigation. For the in vivo study, the prepared calcium phosphate cement was implanted within the calvarium defect. The defects were divided into control versus experimental groups: the control group was CPC implanted in the defect on the left parietal bone. The experimental defect was filled with nanostrontium-enhanced CPC. Also, defects without implanted cements were made in the frontal bone as negative controls. Soft tissues were sutured to achieve primary closure. Four weeks after implantation, the animals were sacrificed. The area of the original surgical defect and the surrounding tissues were removed en bloc and fixed in 10% neutral buffered formalin solution and then decalcified in 10% (v/v) nitric acid. Tissues were embedded in a paraffin block and then serial sectioned using a microtome to slides of approximately 4–6 μm thickness.

Materials Science and Engineering: C, Vol 69 (December 1, 2016): pg. 780-788. DOI.

2.3.8.2.2. Histological analysis and histomorphometry

Slides with tissue sections were de-paraffinized and hydrated through series of xylene and alcohol. The tissue slides were stained with hematoxylin & eosin (H&E) and observed under an optical microscope for the histological observation (E400, Nikon, Tokyo, Japan).

2.3.8.2.3. Radiographic examination

Radiographs were taken using an X-ray machine (Intra Planmeca-Helsinki, Finland), after sacrificing. The percentage of bone formation within the defects was evaluated blindly and independently by two observers.

2.4. Preparation of the composite of simvastatin-loaded poly(lactic-co-glycolic acid) (SIM-loaded PLGA) microspheres plus nanostrontium-CPC

In order to create nanostrontium-CPC-incorporated simvastatin-loaded poly(lactic-*co*-glycolic acid) (SIM-loaded PLGA), first, SIM-loaded PLGA microspheres were produced. The production and evaluation of SIM-loaded PLGA microspheres [without CPC composition] including their simvastatin release kinetics are reported in another article.[34] Briefly put, they were prepared by oil-in-water (O/W) emulsion/solvent evaporation method under magnetic stirrer, and later by centrifuging, and 24 h of freeze drying.[34] Then 3 wt% nanostrontium-CPC was produced as explained above (0.5 g of TTCP with a controlled mean particle size of 10 μm was synthesized and blended with 0.5 g of DCPD, and 3 wt% of synthesized nanostrontium-substituted hydroxyapatite). Afterwards, 0.1 g of SIM-loaded PLGA microspheres was added to the powder cement. Subsequently, for setting of the cement, 1.205 ml (Powder/Liquid = 0.83) of disodium hydrogen phosphate (Na_2HPO_4; Merck) was added to the mixture. The 'SIM-loaded PLGA microspheres + nanostrontium-CPC' composite was vacuum-packed and g-ray-sterilized (20 kGy).

Materials Science and Engineering: C, Vol 69 (December 1, 2016): pg. 780-788. DOI.

2.5. Characterization of the composite of SIM-loaded PLGA microspheres and nanostrontium-CPC

2.5.1. SEM

The composite was scanned as described above.

2.5.2. In vivo evaluations

The efficacy of the produced composite in osteogenesis induction was compared with other biomaterials (3 wt% nanostrontium-enhanced CPC, and 3 wt% nanostrontium-enhanced CPC plus simvastatin) and control groups.

2.5.2.1. Animals, surgical procedures, and experimental groups

Ten mature, male New Zealand white rabbits, with an average weight of 3.5 kg, were purchased from the Pasteur Institute. Each rabbit was housed in an individual cage, in Iranian Tissue Bank and Research, Tehran, Iran. Food and water were available ad libitum. Prophylactic antibiotic (gentamicin 6 mg/kg) was administered 3 h before surgery. The animals were anesthetized with injection of ketamine at a dosage of 40 mg/kg IM (ketamine hydrochloride, Trittau, Germany, Rotexmedica) and Xylazine at a dosage of 5 mg/kg IM (Xylazine 2%, Alfasan-woerden-Holland). During the surgery, lidocaine hydrochloride was locally administered. After shaving and disinfecting the surgical site with 10% pivodine iodine, skin incision was made in dorsal part of the cranium. Then, periosteum was flapped carefully and parietal bone was exposed. Full thickness bone defects, 8 mm in diameter, were parallel trephined in the parietal bone without damaging the dura (trephine height was about the width of the bone). An 8-mm Trephine bur (rotary motor, W&H, Austria) was used to create the defects, under constant irrigation with sterile normal saline to prevent overheating of the bone margins.

In each animal, 5 sites were prepared: a negative control, which was a defect left empty after trephining the bone. A positive control, which was an experimentally made defect, filled with the bone trephined from the site of the negative control. A third defect filled

Materials Science and Engineering: C, Vol 69 (December 1, 2016): pg. 780-788. DOI.

with "SIM-loaded PLGA + nanostrontium-enhanced CPC" composite. A fourth defect filled with 3 wt% nanostrontium-enhanced CPC. And a fifth defect filled with a combination of 3 wt% nanostrontium-enhanced CPC plus simvastatin. The coordinates of defect areas were scaled and noted down.

Afterwards, the periosteum and muscles were carefully repositioned on the outer surface of the implants and sutured in place using catgut 3-0. Afterwards, the skin was sutured with silk 2-0. After the surgery, the rabbits were housed with free access to water and food. Injection with Enrofloxacin 5 mg/kg (Enro-10%, Maghull, Liverpool, UK) was given every 12 h, for 48 h, post-operation. All the experiments and protocols described in the present study were performed in accordance with the guidelines for the care and use of laboratory animals.

2.5.2.2. Histological study and histomorphometry

Animals were euthanized 8 weeks after surgery by vital perfusion, with the intravenous injection of pentobarbital. Defect areas were separated and fixed in 10% formalin for 48 h. Samples were decalcified by 10% formic acid for 30 days, dehydrated in ethanol, and then embedded in 10 × 10-mm paraffin blocks. Samples were then cut into serial 4 μm sections. Three sections from the central area of each defect were selected, stained with H&E, and subjected to histomorphometric analysis. Bone formation was observed under a Nikon light microscope (E400, Tokyo, Japan) at magnification × 400, and analyzed using computerized image processing software.

2.6. Statistical analysis

Data values obtained in the experiments were statistically analyzed by one-way analysis of variance (ANOVA) and Tukey post hoc test. The level of significance was set at 0.05.

3. Results and discussion

Bone defect caused by tumor, trauma and other diseases can often be repaired by bone graft. However, its clinical application is limited due to a second surgical site for access to retrieved graft and

other complications for autogenous bone graft as well as the limited availability, rejection and the spread of disease for allograft. With the development of material and biological science, bone tissue engineering provides a new method to restore the tissue loss or failure, which aims to develop biological substitutes to repair and improve the function of the organization. The basic requirements for an ideal scaffold for bone tissue engineering include several factors as follows.[35,36,37,38] Good biocompatibility: In addition to meet the non-toxic, non-teratogenic and other general requirements, it should be also conducive to the cell adhesion and proliferation, and its degradation products should have no adverse effects on the cell adhesion, growth and differentiation. Good biodegradability: Scaffold material should be degraded after completion of its supporting role, and the degradation should be adapted to the formation of bone tissue, thus contributing to the reconstruction of bone. A 3D porous structure: This structure not only provides a large surface area and space, which is conducive to the growth of cell adhesion, extracellular matrix deposition, nutrients infiltration and metabolite discharge, but also promotes the ingrowth of blood vessels and nerves. Moldability and relatively high mechanical strength: Scaffold material should be formed into a certain shape with a certain mechanical strength, which provides mechanical support for the new tissue and allows for weight bearing. Good osteoconductivity and osteoinductivity: Scaffolds should have surface chemical properties and microstructure to support the bone cell growth and migration.[35,36,37,38]

3.1. Results and discussions pertaining to the nanostrontium-enhanced CPC

3.1.1. XRD analysis

According to diffraction patterns of the prepared samples, TTCP and HA peaks were observed between $0° \leq 2\theta \leq 80°$ with no additional phases such as CaO, perhaps because TTCP was obtained by means of quenching method at 1500 °C after 12 h instead of furnace-cooled method (which might result in production of TTCP, HA and free CaO from decomposition of TTCP).[39] As a result, the optimum process to obtain the high contents of TTCP and remove CaO phase is a quenching after holding 12 h. In additional, it can be concluded that all

the DCPD has transformed into HA in the synthesized cement (Fig. 2). The proportion of powder to liquid is a significant feature of cements as it can affect both bioresorbability and rheological properties.[40] According to the Fig. 2, it seems that by increasing the ratio of Powder/Liquid, crystallinity of the prepared cement might also increase. This might imply an increase in crystallinity of HA in comparison with apatite cements formed in an aqueous environment, which have poorer crystalline HA as the end product.[40] The substitution of calcium with strontium can alter the crystal structure; this is visible in Fig. 2 as well-defined and sharp peaks in association with incorporation of Sr ions. This is in agreement with a high degree of crystallinity of cement reported earlier.[41,42] On the other hand, the broadening is more obvious for the samples with smaller amounts of strontium because there exists a greater difficulty for HA to host the larger Sr ion than for HA-containing Sr to host the smaller calcium ion with respect to their ionic radii (Ca^{2+} ionic radius = 0.100 nm; Sr^{2+} ionic radius = 0.118 nm).[41] Additionally, a shift of diffraction peaks to lower 2θ values with Sr addition was observed; which this might indicate a gradual increase in d-spacing.[42] Meanwhile, in the samples with no strontium hydroxyapatite (Sr-HA), no significant increase in crystallinity was observed.

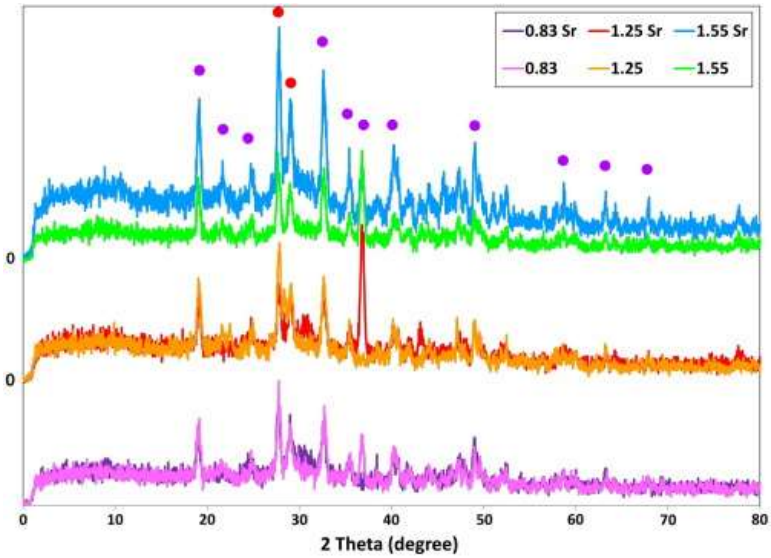

Fig. 2. XRD pattern of CPC and Sr-HA-CPC with different P/L ratios. At 2θ = 0, all the six lines start at zero on the vertical axis. Three P/L ratios have been artificially separated by adding 200 and 400 units to the ratios 1.25 and 1.55, respectively. For each P/L ratio, the results pertaining to CPC and Sr-HA-CPC are overlapped intentionally. Violet circles mark hydroxyapatite. Red circles indicate both hydroxyapatite and tetracalcium phosphate.

3.1.2. FTIR analysis

In Fig. 3, FTIR spectra of the CPC (prepared with and without 3 wt% Sr-HA of different P/L ratios (0.83, 1.25, and 1.55)) are exhibited. There was no considerable difference between CPC with and without strontium. Analyses of the spectra are as follows: FTIR spectra of the three samples follow a single model. The FTIR analysis determines the functional groups of the samples; since the functional groups are similar in all three prepared cements, FTIR similarity is expected. The bands in the range of 3488 to 3497 cm^{-1} spectral of the three types of cements are related to vibration of adsorbed water and presence of hydroxyl groups. Incorporation of Sr ion instead of Ca decreases the relative intensity of the bands of OH^- stretching. In this case vibration modes as well as OH^- stretching mode shift to high wave numbers, while OH^- liberation band shifts to lower wave numbers, in agreement with results reported for Ca-HA and Sr-HA.[43] The bands 1640 to 1643 cm^{-1} are related to absorption of H_2O. The bands at 512–517 cm^{-1}, 520–530 cm^{-1} and 1010–1034 cm^{-1} are related to $V_2PO_4^{-3}$, $V_3PO_4^{-3}$, and $V_1PO_4^{-3}$ respectively that could be due to presence of calcium phosphate compounds (TTCP, DCPD and HA) in the samples. FTIR results of Bigi et al.[41] pertaining to pure Ca-HA showed that phosphate groups shift to lower wave numbers with incorporation of Sr ions and formation Sr-HA. The predominant factor causing the shift in the internal PO_4 frequencies to lower energies is the reduced anion-anion repulsion concomitant with an increased anion-anion separation on increasing cation radius. The influence of Sr in shifting phosphate group is attributed to the increasing average dimensions of the cation,[41] and indicates an increase of irregularity in the HA structure around phosphate sites through the incorporation of Sr. These bands can also be related to formation of hydroxyapatite by the reaction happening between the liquid and powder phases of the cement. The observed bands at 883–881 cm^{-1} are related to carbonate groups; this might imply the absorption of carbonate from the environment.

Materials Science and Engineering: C, Vol 69 (December 1, 2016): pg. 780-788. DOI.

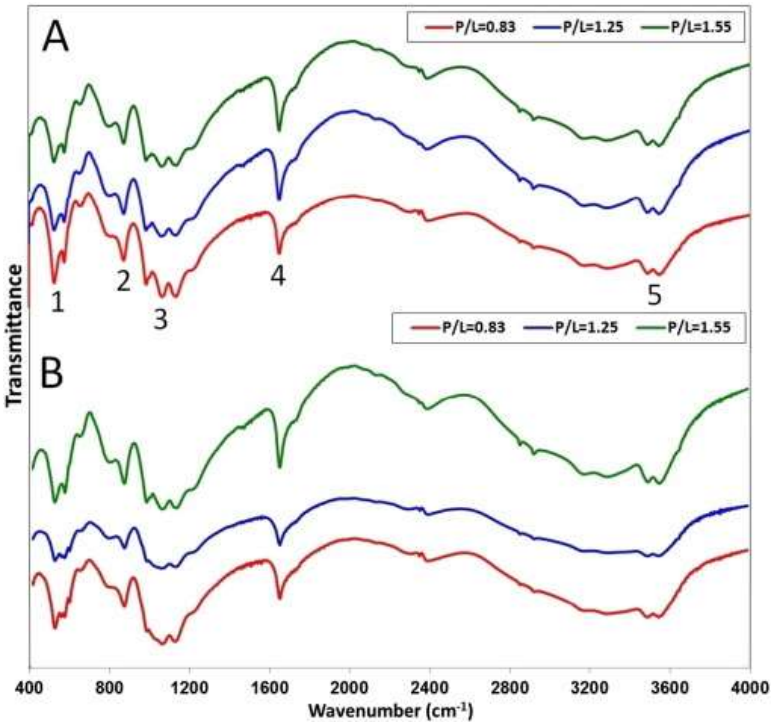

Fig. 3. FTIR spectra of prepared CPC (A) and Sr-HA-CPC (B) with different P/L ratios. 1: $V_2PO_4^{-3}$, 2: carbonate; 3: $V_1PO_4^{-3}$, 4: water; 5: OH.

3.1.3. Thermal analysis

Four phases were observed in thermal analysis. In the first phase (up to 280 °C), the surface humidity is absorbed. The weight reduction of the samples begins at 25 to 280 °C during which about 1 mg of weight is lost, probably as a result of water evaporation. In the second phase, the sample experienced a slight weight loss (about 0.1 mg) in the temperature range of about 280 to 375 °C which can be related to the crystallization of the powders from the amorphous.[44] The third stage (375 to 550 °C) showed about 0.5 mg weight loss, and might be related to reduction of hydroxyl groups with decomposition of HPO_4^{-2} anions to pyrophosphate anions $P_2O_7^{-4}$. The fourth stage (about 2.3 mg weight loss at 550 to 880 °C temperatures) might be attributed to the release of CO_2 gas during endothermic decomposition of CO_3^{-2} and/or decomposition of pyrophosphates to biphasic mixtures [as in $P_2O_7^{4-} \rightarrow 2PO_4^{3-} + H_2O$].[45]

Materials Science and Engineering: C, Vol 69 (December 1, 2016): pg. 780-788. DOI.

3.1.4. SEM observations

The SEM micrographs of CPC and Sr-HA-CPC (Fig. 4) indicate that with increasing the P/L ratio, the formation of hydroxyapatite crystals (arising from the interaction of solid and liquid phases) might decrease. The incorporation of Sr within Ca site causes a dramatic increase in crystallinity of hydroxyapatite. Strontium atoms can occupy both M(1) and M(2) sites of the apatite structure, depending on the amount of strontium. At very low Sr contents, the occupancy of M(1) is more probable, while samples containing > 10 atom% Sr demonstrated a preferential Sr occupancy at M(2) sites.[41] The M(2) sites allow a better accommodation of the bigger Sr atoms; whereas in the M(1) sites, metals are hardly aligned in columns parallel to the c-axis. Perhaps, longer average M(1)-O distances might allow the accommodation of a larger cation. With increase of the number of bigger ions, the repulsion between atoms in the M(1) site might trigger an enlargement of the c-axis. Furthermore, the greater extent of Sr distribution might cause a significant discontinuity in the cell parameter variation.[46] It was also reported that within each specific Sr occupancy, the relationship between the excess energies E_x of the solid solution Sr-HA-X structures and sites for substitution of Sr is E_x site (1) < E_x mixed sites < E_x site (2). Hence, Sr incorporation at site 1 is more favorable than at mixed sites followed by site 2.[47]

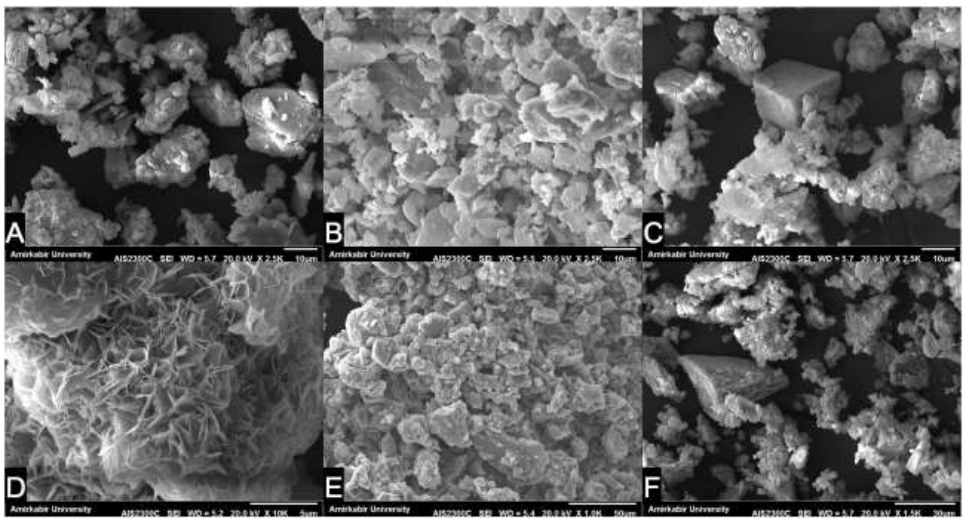

Fig. 4. SEM micrographs of prepared CPC without 3 wt% Sr-HA (A to C) and with 3 wt% Sr-HA (D to F). The P/L ratios are 0.83, 1.25 and 1.55, from left to right (i.e., from A to C, and from D to F).

Materials Science and Engineering: C, Vol 69 (December 1, 2016): pg. 780-788. DOI.

3.1.5. Setting time

With an increase in the powder-to-liquid ratio of 3 wt% Sr-HA-CPC, the setting time might reduce (Table 1). The relative solubility of phases of TTCP and DCPD is regarded as a major factor affecting the setting time of calcium phosphate. HA was precipitated according to the following equation: $2Ca_4(PO)_2O + 2CaHPO_4 \rightarrow Ca_{10}(PO_4)_6(OH)_2$.

Table 1. Setting time of the prepared CPC with 3 wt% Sr-HA with different P/L ratio.

P/L ratio	Setting time (min)
0.83	28.7±0.4
1.25	9.3±0.1
1.55	2.2±0.2

Applying Na_2HPO_4 (as a liquid phase) to prepare the cement increases the rate of hydroxyapatite formation and decreases the setting time. In other words, lower powder-to-liquid ratios might elongate the working and setting time of the mass, delaying the supersaturation of hydrate phases (i.e., hydroxyapatite In apatite cements).[48]

3.1.6. ICP analysis

The release of strontium after interaction in the Sr-free medium is presented for cement samples in Table 2. This might be useful for osteoporosis therapy.[49,50] The smooth delivery of Sr^{2+} ions in biological conditions might be attributed to the substitution of Ca for Sr in the Sr-enhanced cements.[49,51] After this interaction, some strontium remains in the hydroxyapatite and might serve as a reservoir for future osseointegration of implants upon bone re-modeling.[49,51]

Table 2. Release of Sr, Ca and P ions as a function of interaction time for cement samples (P value < 0.01).

Days	Ca (ppm)	P (ppm)	Sr (ppm)
10	39.6±4.7	60.9±3.6	0.1
20	62.8±8.9	70.2±7.7	0.3±0.1
110	138.6±13.4	121.8±15.8	0.8±0.1

3.1.7. Mechanical properties

Mechanical properties of the cement are given in Fig. 5. Although the ceramic samples behaved similar to other ceramic bone cements but their mechanical properties were smaller compared to their corresponding values in spongy and compact bone.

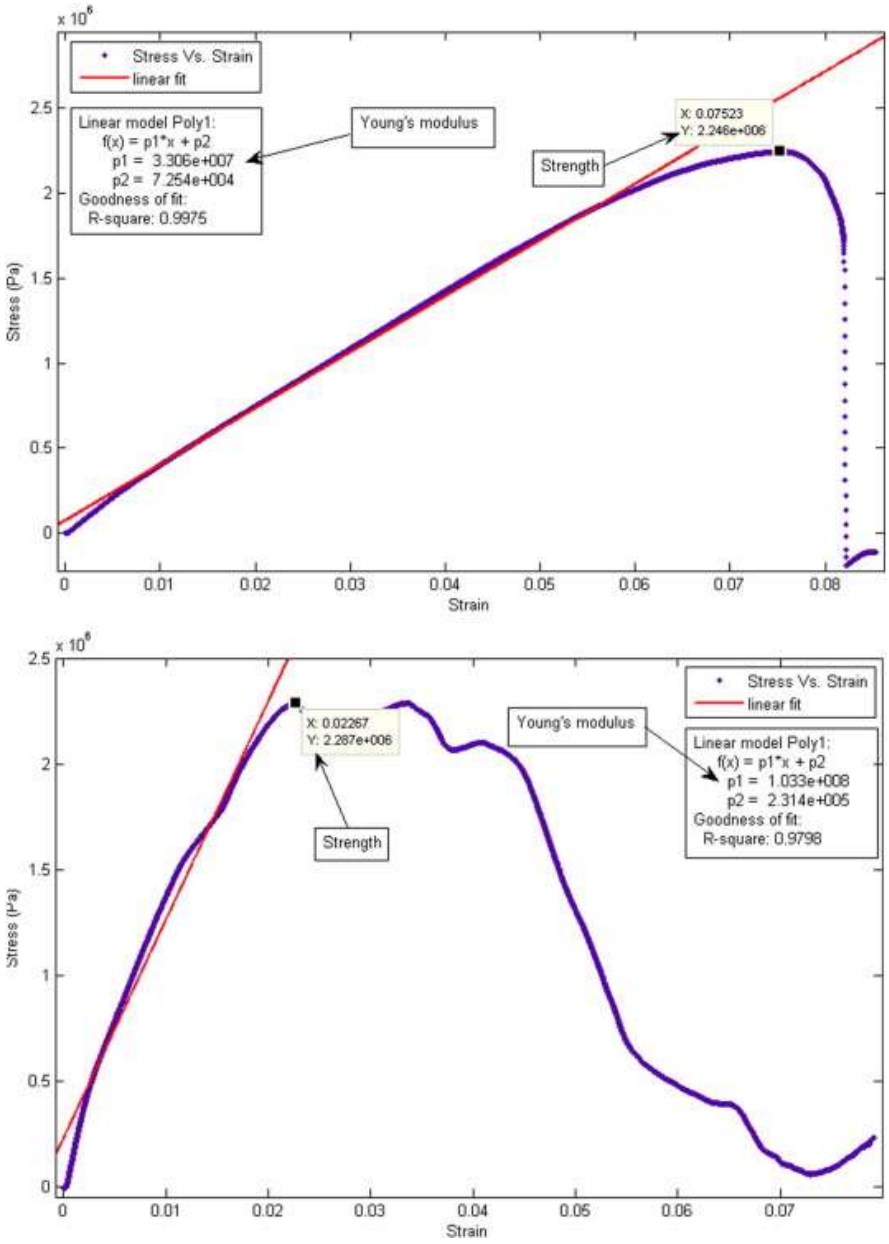

Fig. 5. Mechanical properties of the prepared cement. The final amounts of the Young's modulus and ultimate strength are 33.06 ± 2.06 and 2.24 ± 0.12 MPa, respectively.

Materials Science and Engineering: C, Vol 69 (December 1, 2016): pg. 780-788. DOI.

3.1.8. Biological evaluations

3.1.8.1. In vitro study

3.1.8.1.1. MTT assay

Cytocompatibility of the prepared cements was assessed using MTT assay (Fig. 6). After 14 days of incubation, the cell viability decreased for all samples, whereas, the reduction was insignificant for all of them. Addition of 3 wt% of nanostrontium hydroxyapatite (Sr-HA) increased the biocompatibility of the prepared cements ($P < 0.05$). The prepared cements have proper biocompatibility and are suitable for use as bone cement. It has been proved that Sr ions can stimulate cellular responses. The influence of strontium ions on viability of osteoblastic cells might be dose-dependent, owing to the lower viability rate of the osteoblasts on calcium phosphate cements compared with their viability on other Sr-hydroxyapatite cements. In agreement with other studies, our findings as well indicated that the incorporation of Sr in hydroxyapatite cement might encourage new bone formation.[42,52] Although, it is known that Sr incorporation enhances cell proliferation, its optimum concentration is still controversial. Park et al.[53] found that Sr ions release at 103–135 ppb increased the differentiation of osteoblast. Also, other results suggest that Sr alone at concentrations between 1.21 and 3.24 does not impact the proliferation of osteoblast cells.[42]

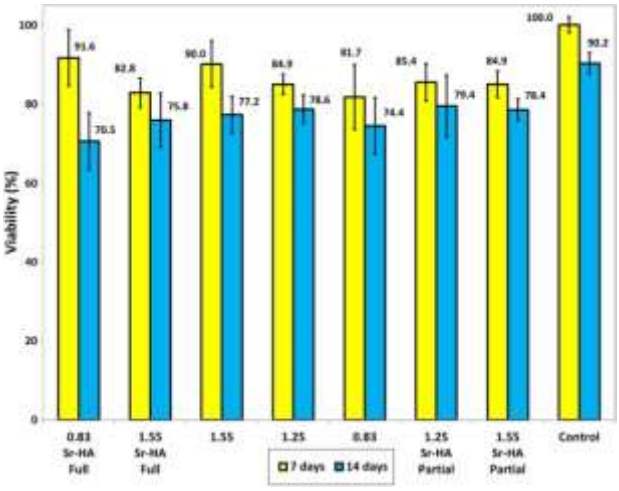

Fig. 6. Cell proliferation of SAOS-2 cells proliferated on the CPC with and without 3 wt% Sr-HA with different P/L ratios along with negative control after incubation for 7, and 14 days.

Materials Science and Engineering: C, Vol 69 (December 1, 2016): pg. 780-788. DOI.

3.1.8.1.2. Alkaline phosphatase

Measurement of ALP activity is considered one of the criteria necessary for osteoblast activity. Fig. 7 shows the results of the ALP activity of different prepared cements after 3 and 7 days of incubation, indicating a significant increase in ALP activity by adding Sr-HA ($P < 0.05$). This might be attributed to the presence of strontium ions which might increase the activity of bone cells. The cements with P/L ratio of 1.25 had the highest level of alkaline phosphatase activity compared to P/L ratios of 1.55 and 0.83. Therefore, the P/L ratio of 1.25 was selected as the optimum ratio in CPC. It is noteworthy that the biology activity of Sr-containing cement is also attributed to the influences on crystallinity and expansion of its crystal lattice due to the larger size of Sr compared to Ca. In addition, according to the SEM analysis (Fig. 4), the samples containing Sr consisted of larger, needle-like crystals. As a result, the small tightly entangled crystal can provide more nucleation sites for the formation of apatite crystals.[54,55]

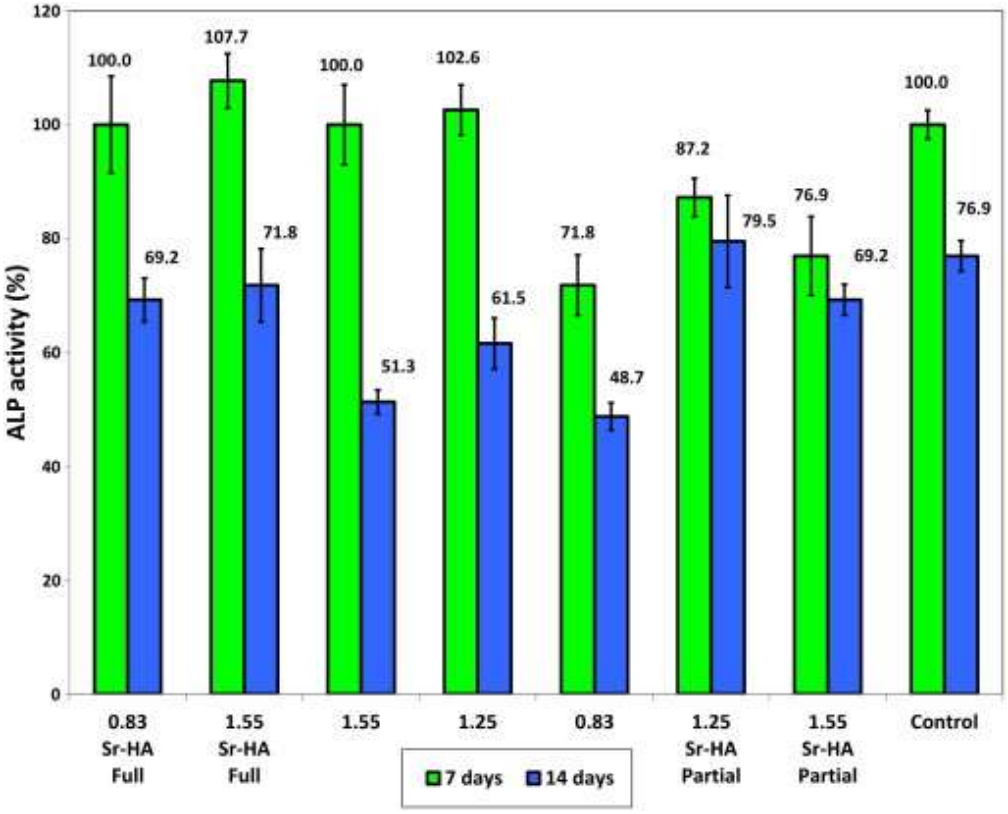

Fig. 7. ALP activity test for SAOS-2 cells proliferated on the CPC with and without 3 wt% Sr-HA with different P/L ratio along with negative control after incubation for 7 and 14 days ($P > 0.05$).

3.1.8.2. In vivo study

3.1.8.2.1. Histological analysis and histomorphometry

The in vivo bone tissue response towards three samples was evaluated by means of histological examination, after surgical placement of the materials "3 wt% Sr-HA/CPC", "CPC" and the control in rat for 4 weeks (Fig. 8). After 4 week post-implantation, no severe inflammation, tissue necrosis or tissue rejection was observed. Generally, fibrous connective tissue and blood vessels grow into the macropores, contributing to the early fixation of the samples.

Fig. 8. Implantation steps in rat (the frontal socket is negative control).

CPC gradually dissolves in the body and releases calcium and phosphate ions.[56] The histomorphometric analysis in this study displayed an increase in the bone formation for the Sr-CPC (ANOVA's $P < 0.05$) in comparison with the defect areas filled with CPC without Sr and the negative control (empty defect). It should also be noted that the formation of bone at both the periphery and center of fracture defect area for all the samples were visible. This can be attributed to the local release of Sr from cement that might improve osteogenesis. Molecular-biological activities (enhanced expression of BMP2, osteocalcin and OPG) were observed in this study indicating an increased formation of new bone in Sr-containing cement in comparison with CPC and the negative control. Furthermore, it is

Materials Science and Engineering: C, Vol 69 (December 1, 2016): pg. 780-788. DOI.

possible that strontium's osteogenic activity preserved within the cement.[25,57] The uptake of strontium by the bone may increase the bone volume by increasing the sites of bone formation and decreasing bone resorption, without affecting the rate of osteogenesis and bone mineralization.[54]

3.1.8.2.2. Radiographic analysis

Strontium-containing cement is inherently radiopaque without a need to additional materials for radio-examination. No inflammatory response and no necrosis were found in the rats implanted with Sr-HA cement. The similarity of minerals in Sr-HA cement and bone promotes the fusion of the material to the bone during osteogenesis. As a consequence, Sr-HA bioactive cement might have the potential to be utilized to treat osteoporotic fractures.[58]

3.2. Results and discussions pertaining to the composition of SIM-loaded PLGA microspheres + nanostrontium-enhanced CPC

3.2.1. SEM observations

Materials Science and Engineering: C, Vol 69 (December 1, 2016): pg. 780-788. DOI.

The SIM-PLGA + Sr-PC scaffold possessed suitable pore sizes and interconnected pores (Fig. 9).

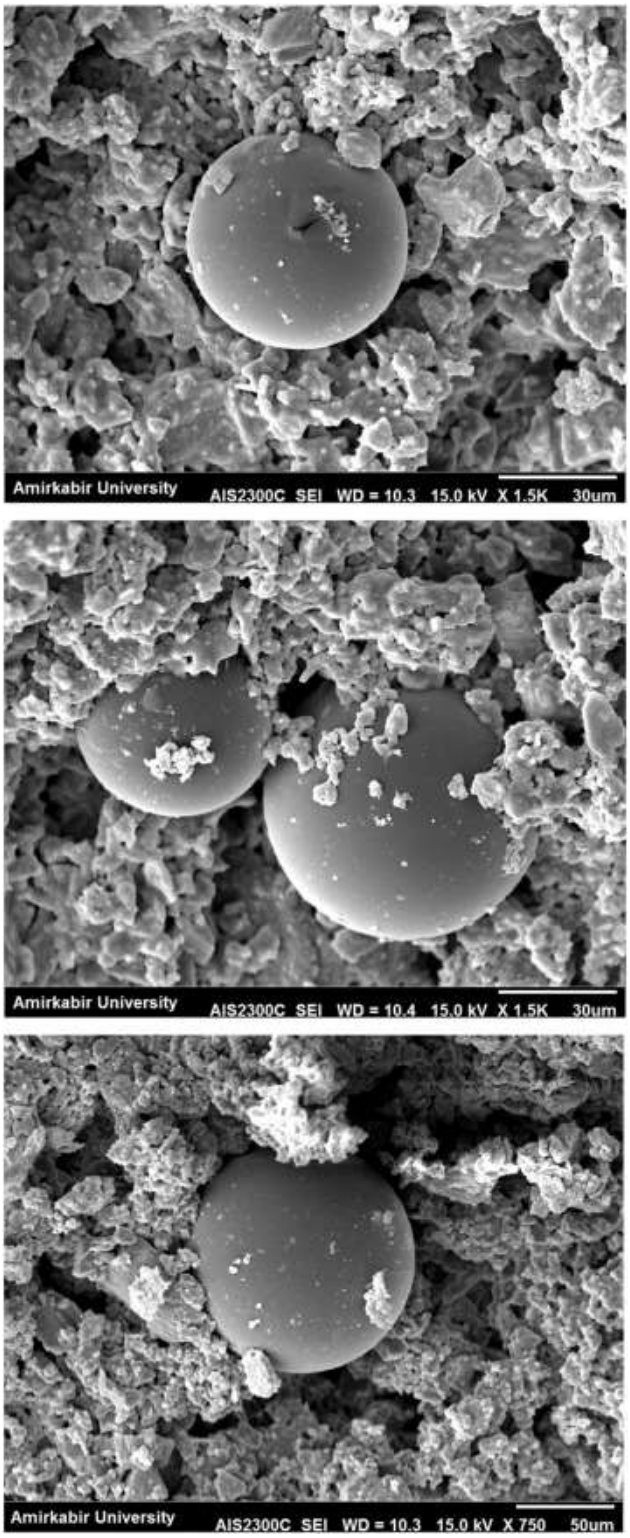

Materials Science and Engineering: C, Vol 69 (December 1, 2016): pg. 780-788. DOI.

Fig. 9. SEM micrographs of cement containing SIM-loaded PLGA.

3.2.2. In vivo evaluations

The surgical steps for rabbit are presented in Fig. 10. After 8 weeks of in vivo application, only a small amount of bone had been regenerated in the control group (Fig. 11). This newly formed bone was only localized at the boundary of the defect, and the defects were mostly filled with soft tissue. On the other hand, the other groups showed new bone formation within the bone cements filling the defect. The new bone area for the control group was significantly lower than the other groups (Tukey's $P < 0.01$). A significant difference was found in the osteogenesis induced by the groups sham (negative) control (16.96 ± 1.01), bone materials (positive control) (32.28 ± 4.03), nanostrontium-CPC (24.84 ± 2.6), nanostrontium-CPC-simvastatin (40.12 ± 3.29), and SIM-loaded PLGA + nanostrontium-CPC (44.8 ± 6.45) (ANOVA's $P < 0.001$). All the pairwise comparisons were significant (Tukey's $P < 0.01$), except that of nanostrontium-CPC-simvastatin and SIM-loaded PLGA + nanostrontium-CPC. This confirmed the efficacy of the SIM-loaded PLGA + nanostrontium-CPC composite, and its superiority over all materials except SIM-containing nanostrontium-CPC (Table 3). SIM is widely used in clinical lipid-lowering drugs, and its osteogenic potential for bone metabolism has become a hot research field in recent years.[28,32,33] SIM plays a role in promoting new bone formation and regulation, which is related to BMP-2 and VEGF expression of osteoblasts.[21,22] In our study, we found the scaffolds co-cultured with BMSCs in vitro improved the cell proliferation and significantly induced osteogenic differentiation, thus promoting the ALP activity and enhancing their osteogenic capability. Drug utilization rate of systemic administration is limited due to its potential systemic side effects. Topical administration makes a higher drug concentration at the bone defect site, leading to suppressed drug utilization rate.[23] The results of the in vivo experiments showed that the pure CPC group had the least new bone formation area at 8 weeks after implantation. However, the new bone formation area of SIM-loaded group was significantly higher than other groups, indicating that of topical administration in vivo and satisfactory osteogenic effect could be obtained through the application of SIM-PLGA + Sr-CPC scaffold. Pore size and porosity of the scaffold are important conditions for ingrowth of new bone tissue, and it is desirable to provide a

suitable pore space for the bone formation, vascular ingrowth and deposition of extracellular matrix. Osteoblast migration requires a minimum pore size of 100 μm, whereas a suitable fibroblast growing space is 180–300 μm.[24,25] Therefore, in order to provide the most basic environment of osteoblast growth, the pore size of scaffolds should be around 200 μm. However, only a suitable pore size is not enough for porous scaffold material.[26] It is difficult to cause the new bone to grow inside the scaffold if the connection between the porosity is not sufficient. The interconnected micropores on the pore walls of macropores are conducive to new blood vessels to grow deeper into the scaffold, to supply nutrients and discharge metabolites, which is beneficial to the new bone formation. In the present study, in vitro methods were adopted to test the response of BMSCs to the SIM-PLGA + Sr-CPC scaffold. The results suggested that SIM-PLGA + Sr-CPC scaffolds promoted a higher degree of osteogenic differentiation compared with pure scaffolds. It also indirectly indicated that SIM could play a role in promoting the osteogenic differentiation of BMSCs. During our investigation, all rabbits were under good health and did not show any surgery complications. At 8 weeks, the implanted SIM-PLGA + Sr-CPC scaffolds and tissue cells exhibited good biocompatibility. Radiographic and histological investigations were performed to assess the process of bone tissue formation.

Fig. 10. The surgical steps in rabbit (the first row), and the outcome (the second row).

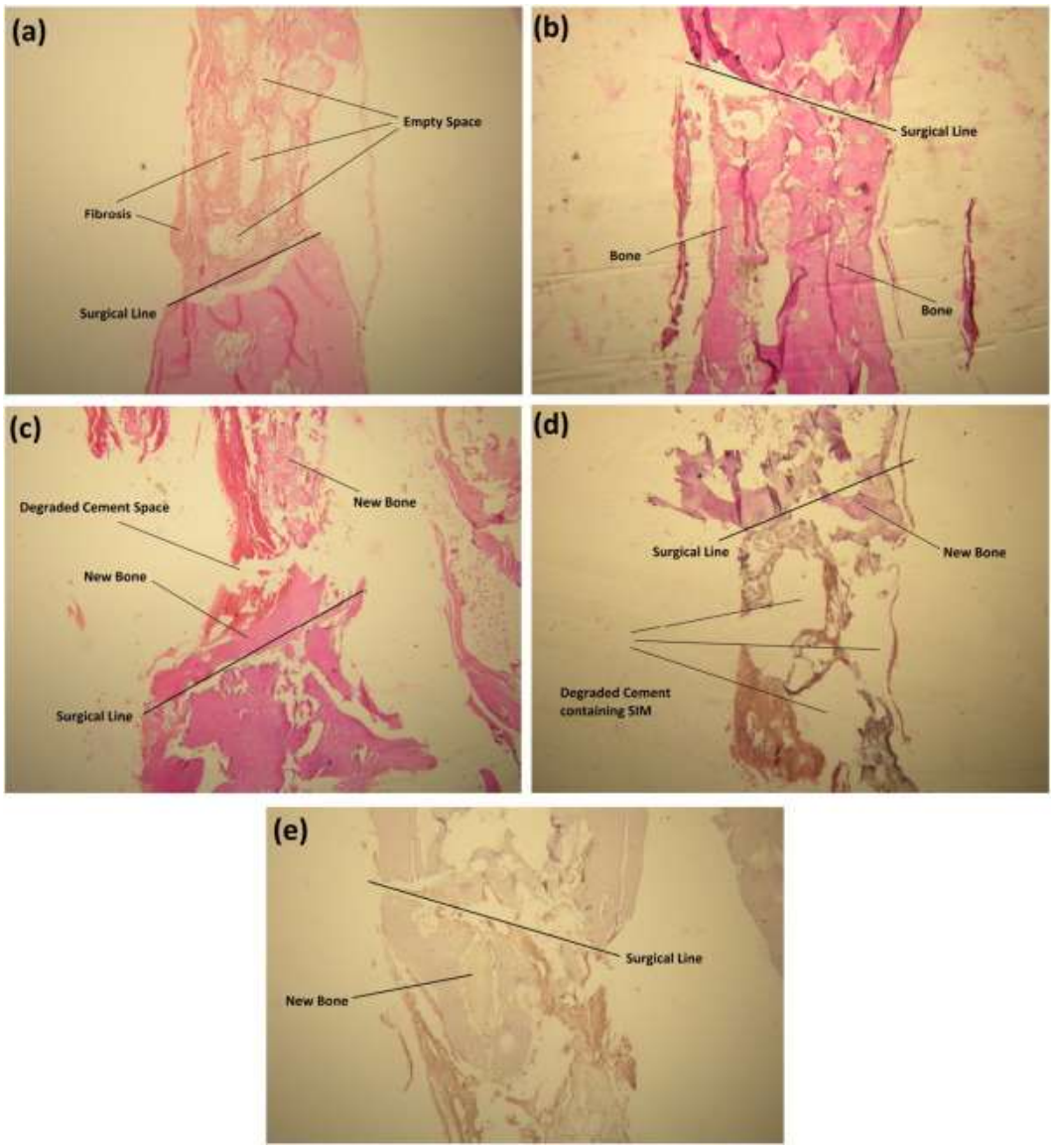

Fig. 11. Histological images at 8 weeks, (a) no augmentation (control group; ctrl), (b) bone materials (BM), (c) Sr-CPC (C), and (d) Sr-CPC containing SIM (CS) and (e) Sr-CPC containing SIM loaded PLGA microsphere (CPS).

Table 3. New bone formation (%) in rabbit.

Groups	Mean	SD	95% CI	
Negative control	16.96	1.01	16.33	17.59
Bone materials	32.28	4.03	29.78	34.78
Sr-CPC	24.84	2.60	23.23	26.45
Sr-CPC+SIM	40.12	3.29	38.08	42.16
Sr-CPC-SIM-PLGA	44.80	6.45	40.80	48.80

This study also had limitations. Young animals have better physical condition as well as more resistance to operation compared to old ones. Therefore, only young animals were included. This may limit the clinical relevance of the results. Moreover, it was better to test a broader range of powder-to-liquid ratios, in order to identify the optimized ratio with a greater confidence. In addition, SEM interpretation is subjective and prone to bias.

4. Conclusions

4.1. Nanostrontium-enhanced CPC

In conclusion, XRD analysis demonstrated that by increasing the ratio of powder-to-liquid, crystallinity of the prepared cement increases. The substitution of calcium by strontium in CPC can alters the crystal structure. According to the SEM observations, by increasing the P/L ratio of CPC, the formation of hydroxyapatite crystals arising from the interaction of solid and liquid phase of cement will be reduced. Sr-CPC has better ALP activity and biocompatibility (indicated by MTT assay) and induced higher bone regeneration.

4.2. SIM-loaded PLGA microspheres + nanostrontium-enhanced CPC

The prepared composite exhibited a good interconnective pore structure for cell seeding and transplantation. Sr-CPC containing simvastatin-loaded PLGA microsphere demonstrated a higher level of osteogenic differentiation.

The key findings of this study can be summarized as follows. The addition of nanostrontium can enhance the chemophysical properties of CPC and increase the crystallinity of hydroxyapatite while being cytocompatible and encouraging osteogenesis without inducing inflammatory responses or other disturbances for the tissue. Higher P/L ratios of nano-Sr-CPC might improve the chemomechanical properties and reduce the setting time. The composition of nano-Sr-CPC with PLGA microsphere loaded with simvastatin creates a porous material that can boost the osteogenesis about twice compared to the osteogenesis induced by nano-Sr-CPC.

Materials Science and Engineering: C, Vol 69 (December 1, 2016): pg. 780-788. DOI.

Acknowledgements

This research has been supported by Tehran University of Medical Sciences and Health Services grant no. 92-03-69-24058.

References

[1]R.K. Duffy, A.B. Shafritz. Bone cement. *J. Hand Surg. Eur. Vol.,* 6 (36(6)) (2011), pp. 1086–1088

[2]M.P. Ginebra. 10 — calcium phosphate bone cements. S. Deb (Ed.), *Orthopaedic Bone Cements,* Woodhead Publishing (2008), pp. 206–230

[3]M.P. Ginebra, T. Traykova, J.A. Planell. Calcium phosphate cements as bone drug delivery systems: a review. *J. Control. Release.,* 113 (2) (6/28/2006), pp. 102–110

[4]R. Vaishya, M. Chauhan, A. Vaish. Bone cement. *J. Clin. Orthopaedics and Trauma,* 12 (4(4)) (2013), pp. 157–163

[5]T.J. Keane, S.F. Badylak. Biomaterials for tissue engineering applications. *Semin. Pediatr. Surg.,* 6 (23(3)) (2014), pp. 112–118

[6]I. Kulinets. 1 — biomaterials and their applications in medicine. A. SF, R.M. Ezzell (Eds.), *Regulatory Affairs for Biomaterials and Medical Devices,* Woodhead Publishing (2015), pp. 1–10

[7]M.-P. Ginebra, C. Canal, M. Espanol, D. Pastorino, E.B. Montufar. Calcium phosphate cements as drug delivery materials. *Adv. Drug Deliv. Rev.,* 9 (64(12)) (2012), pp. 1090–1110

[8]L.D.T. Topoleski, R.-P. R. 6.602 — bone cement. P. Ducheyne (Ed.), *Comprehensive Biomaterials*, Elsevier, Oxford (2011), pp. 11–28

[9]R.E. Bauer. Novel calcium phosphate cement based scaffolds for bone tissue engineering. *J. Oral Maxillofac. Surg.,* 9 (68(9, Supplement) (2010), pp. e49–e50

[10]C. Canal, M.P. Ginebra. Fibre-reinforced calcium phosphate cements: a review. *J. Mech. Behav. Biomed. Mater.,* 11 (4(8)) (2011), pp. 1658–1671

[11]R. Krüger, J. Groll. Fiber reinforced calcium phosphate cements — on the way to degradable load bearing bone substitutes? *Biomaterials,* 9 (33(25)) (2012), pp. 5887–5900

[12]S. Larsson. 17 — clinical aspects of calcium phosphate bone cements. S. Deb (Ed.), *Orthopaedic Bone Cements*, Woodhead Publishing (2008), pp. 377–400

[13]Z. Shen, T. Yu, J. Ye. Microstructure and properties of alendronate-loaded calcium phosphate cement. *Mater. Sci. Eng. C,* 42 (0) (9/1/2014), pp. 303–311

[14]A. Shiotani, K. Saito, T. Fujimine, K. Okubo, M. Tomifuji. P074: injection laryngoplasty using calcium phosphate cement. *Otolaryngol. Head Neck Surg.,* 8 (137(2, Supplement)) (2007), p. P237

[15]C. Cao, H. Li, J. Li, C. Liu, H. Yang, B. Li. Mechanical reinforcement of injectable calcium phosphate cement/silk fibroin (SF) composite by mineralized SF. *Ceram. Int.,* 11 (40(9, Part A)) (2014), pp. 13987–13993

[16]C.-T. Kao, T.-H. Huang, Y.-J. Chen, C. Hung Jr., C.-C. Lin, M.-Y. Shie. Using calcium silicate to regulate the physicochemical and biological properties when using β-tricalcium phosphate as bone cement. *Mater. Sci. Eng. C,* 43 (0) (10/1/2014), pp. 126–134

[17]S. Larsson, S. VA, J. Arnoldi, M. Behrens, B. Hess, P. Procter, *et al.* Injectable calcium phosphate cement for augmentation around cancellous bone screws. In vivo biomechanical studies. *J. of Biomechanics,* 45 (7) (4/30/2012), pp. 1156–1160

[18]L.A. Vasconcellos, L.A. dos Santos. Calcium phosphate cement scaffolds with PLGA fibers. *Mater. Sci. Eng. C,* 33 (3) (4/1/2013), pp. 1032–1040

[19]D. Meng, L. Dong, Y. Wen, Q. Xie. Effects of adding resorbable chitosan microspheres to calcium phosphate cements for bone regeneration. *Mater. Sci. Eng. C,* 47 (0) (2/1/2015), pp. 266–272

[20]R. O'Hara, F. Buchanan, N. Dunne. 2 — injectable calcium phosphate cements for spinal bone repair. P. Dubruel, V. SV (Eds.), *Biomaterials for Bone Regeneration*, Woodhead Publishing (2014), pp. 26–61

[21]S.D. Blaschko, T. Chi, J. Miller, L. Flechner, S. Fakra, P. Kapahi, *et al.* Strontium substitution for calcium in lithogenesis. *J. Urol.,* 2 (189(2)) (2013), pp. 735–739

[22]J. Cabrejos-Azama, M.H. Alkhraisat, C. Rueda, J. Torres, L. Blanco, E. López-Cabarcos. Magnesium substitution in brushite cements for enhanced bone tissue regeneration. *Mater. Sci. Eng. C,* 43 (0) (10/1/2014), pp. 403–410

[23]M. Huang, T. Li, N. Zhao, Y. Yao, H. Yang, C. Du, *et al.* Doping strontium in tricalcium phosphate microspheres using yeast-based biotemplate. *Mater. Chem. Phys.,* 147 (3) (10/15/2014), pp. 540–544

[24]V. Sternitzke, M. Janousch, M.B. Heeb, J.G. Hering, C.A. Johnson. Strontium hydroxyapatite and strontium carbonate as templates for the precipitation of calcium-phosphates in the absence and presence of fluoride. *J. Cryst. Growth.,* 396 (0) (6/15/2014), pp. 71–78

[25]U. Thormann, S. Ray, U. Sommer, T. ElKhassawna, T. Rehling, M. Hundgeburth, *et al.* Bone formation induced by strontium modified calcium phosphate cement in critical-size metaphyseal fracture defects in ovariectomized rats. *Biomaterials,* 11 (34(34) (2013), pp. 8589–8598

[26]R. Drevet, H. Benhayoune. Pulsed electrodeposition for the synthesis of strontium-substituted calcium phosphate coatings with improved dissolution properties. *Mater. Sci. Eng. C,* 10 (33(7)) (2013), pp. 4260–4265

[27]E.R. Balmayor, K. Tuzlakoglu, A.P. Marques, H.S. Azevedo, R.L. Reis. A novel enzymatically-mediated drug delivery carrier for bone tissue engineering applications: combining biodegradable starch-based microparticles and differentiation agents. *J. Mater. Sci. Mater. Med.,* 19 (4) (01/24/2008), pp. 1617–1623 2008

[28]T.-Q. Bao, N.-T. Hiep, Y.-H. Kim, H.-M. Yang, L. B-T. Fabrication and characterization of porous poly(lactic-*co*-glycolic acid) (PLGA) microspheres for use as a drug delivery system. *J. Mater. Sci.,* 46 (8) (12/03/2010) 2010. 2510–7

[29]Y.S. Choi, S.-N. Park, H. Suh. Adipose tissue engineering using mesenchymal stem cells attached to injectable PLGA spheres. *Biomaterials,* 29 (10/26/2005), pp. 5855–5863 2005

[30]Y.-Y. Yang, T.-S. Chung, N.P. Ng. Morphology, drug distribution, and in vitro release profiles of biodegradable polymeric microspheres containing protein fabricated by double-emulsion solvent extraction/evaporation method. *Biomaterials,* 22 (3) (2001), pp. 231–241

[31]R. Herrero-Vanrell, L. Ramirez, A. Fernandez-Carballido, M.F. Refojo. Biodegradable PLGA microspheres loaded with ganciclovir for intraocular administration. Encapsulation technique, in vitro release profiles, and sterilization process. *Pharm. Res.,* 17 (10) (2000 Oct), pp. 1323–1328

[32]J.H. Jeon, M.V. Thomas, D.A. Puleo. Bioerodible devices for intermittent release of simvastatin acid. *Int. J. Pharm.,* 340 (1–2) (2007 Aug 1), pp. 6–12

[33]R. Hu, J. Zhu, G. Chen, Y. Sun, K. Mei, S. Li. Preparation of sustained-release simvastatin microspheres by the spherical crystallization technique. *Asian J. Pharm Sci.,* 1 (2006), pp. 47–52

[34]R. Masaeli, J. Kashi, T. Sadat, R. Dinarvand, M. Tahriri, V. Rakhshan, *et al.* Preparation, characterization and evaluation of drug release properties of simvastatin-loaded PLGA microspheres. *Iran. J. Pharm. Res.,* 15 (2016), pp. 205–211

[35]A. Shiotani, K. Saito, T. Fujimine, K. Okubo, M. Tomifuji. P074: injection laryngoplasty using calcium phosphate cement. *Otolaryngol. Head Neck Surg,* 137 (2 suppl) (2007) P237-P

[36]C. Cao, H. Li, J. Li, C. Liu, H. Yang, B. Li. Mechanical reinforcement of injectable calcium phosphate cement/silk fibroin (SF) composite by mineralized SF. *Ceram. Int.,* 40 (9) (2014), pp. 13987–13993

[37]C.-T. Kao, T.-H. Huang, Y.-J. Chen, C.-J. Hung, C.-C. Lin, M.-Y. Shie. Using calcium silicate to regulate the physicochemical and biological

properties when using β-tricalcium phosphate as bone cement. *Mater. Sci. Eng. C,* 43 (2014), pp. 126–134

[38]L. Chen, W.-M. Zhu, Z.-Q. Fei, J.-L. Chen, J.-Y. Xiong, J.-F. Zhang, *et al.* The study on biocompatibility of porous nHA/PLGA composite scaffolds for tissue engineering with rabbit chondrocytes in vitro. *BioMed. Res. Int.,* 2013 (2013), p. 412745

[39]C. Jeon, S. Chun, S. Lim, S. Kim. Synthesis and characterization of TTCP for calcium phosphate bone cement. *Biomaterials Res.,* 15 (1) (2011), pp. 1–6

[40]S.V. Dorozhkin. Calcium orthophosphate cements and concretes. *Materials,* 2 (1) (2009), pp. 221–291

[41]A. Bigi, E. Boanini, C. Capuccini, M. Gazzano. Strontium-substituted hydroxyapatite nanocrystals. *Inorg. Chim. Acta.,* 360 (3) (2/15/2007), pp. 1009–1016

[42]V. Aina, L. Bergandi, G. Lusvardi, G. Malavasi, F.E. Imrie, I.R. Gibson, *et al.* Sr-containing hydroxyapatite: morphologies of HA crystals and bioactivity on osteoblast cells. *Mater. Sci. Eng. C Mater. Biol. Appl.,* 33 (3) (2013 Apr 1), pp. 1132–1142

[43]B. Fowler. Infrared studies of apatites. I. Vibrational assignments for calcium, strontium, and barium hydroxyapatites utilizing isotopic substitution. *Inorg. Chem.,* 13 (1) (1974), pp. 194–207

[44]A process for the development of strontium hydroxyapatite. N. Zahra, M. Fayyaz, W. Iqbal, M. Irfan, S. Alam (Eds.), *IOP Conference Series: Materials Science and Engineering,* IOP Publishing (2014)

[45]S. Lazić, S. Zec, N. Miljević, S. Milonjić. The effect of temperature on the properties of hydroxyapatite precipitated from calcium hydroxide and phosphoric acid. *Thermochim. Acta,* 374 (1) (2001), pp. 13–22

[46]M. Kikuchi, A. Yamazaki, R. Otsuka, M. Akao, H. Aoki. Crystal structure of Sr-substituted hydroxyapatite synthesized by hydrothermal method. *J. Solid State Chem.,* 12 (113(2)) (1994), pp. 373–378

[47]J. Terra, E.R. Dourado, J.-G. Eon, D.E. Ellis, G. Gonzalez, A.M. Rossi. The structure of strontium-doped hydroxyapatite: an experimental and theoretical study. *Phys. Chem. Chem. Phys.,* 11 (3) (2009), pp. 568–577

[48]J. Shahrouzi, S. Hesaraki, A. Zamanian. The effect of paste concentration on mechanical and setting properties of calcium phosphate bone cements. *Adv. Chem. Eng. Res. Bull.* (2012)

[49]G. Renaudin, P. Laquerriere, Y. Filinchuk, E. Jallot, J.-M. Nedelec. Structural characterization of sol–gel derived Sr-substituted calcium phosphates with anti-osteoporotic and anti-inflammatory properties. *J. Mater. Chem.,* 18 (30) (2008), pp. 3593–3600

Materials Science and Engineering: C, Vol 69 (December 1, 2016): pg. 780-788. DOI.

[50]S. Dahl, P. Allain, P. Marie, Y. Mauras, G. Boivin, P. Ammann, *et al.* Incorporation and distribution of strontium in bone. *Bone,* 28 (4) (2001), pp. 446–453

[51]M. Yashima, A. Sakai, T. Kamiyama, A. Hoshikawa. Crystal structure analysis of β-tricalcium phosphate $Ca_3(PO_4)_2$ by neutron powder diffraction. *J. Solid State Chem.,* 175 (2) (2003), pp. 272–277

[52]A. Pouria, H. Bandegani, M. Pourbaghi-Masouleh, S. Hesaraki, M. Alizadeh. Physicochemical properties and cellular responses of strontium-doped gypsum biomaterials. *Bioinorg. Chem. Appl.,* 2012 (2012)

[53]J.W. Park, Y.J. Kim, J.H. Jang. Enhanced osteoblast response to hydrophilic strontium and/or phosphate ions-incorporated titanium oxide surfaces. *Clin. Oral Implants Res.,* 21 (4) (2010), pp. 398–408

[54]S.J. Saint-Jean, C. Camire, P. Nevsten, S. Hansen, M. Ginebra. Study of the reactivity and in vitro bioactivity of Sr-substituted α-TCP cements. *J. Mater. Sci. Mater. Med.,* 16 (11) (2005), pp. 993–1001

[55]S. Pina, P. Torres, J. Ferreira. Injectability of brushite-forming Mg-substituted and Sr-substituted α-TCP bone cements. *J. Mater. Sci. Mater. Med.,* 21 (2) (2010), pp. 431–438

[56]D. Bizari, F. Moztarzadeh, M. Rabiee, M. Tahriri, F. Banafatizadeh, A. Ansari, *et al.* Development of biphasic hydroxyapatite/dicalcium phosphate dihydrate (DCPD) bone graft using polyurethane foam template: in vitro and in vivo study. *Adv. Appl. Ceram.,* 110 (7) (2011), pp. 417–425

[57]O.Z. Andersen, V. Offermanns, M. Sillassen, K.P. Almtoft, I.H. Andersen, S. Sørensen, *et al.* Accelerated bone ingrowth by local delivery of strontium from surface functionalized titanium implants. *Biomaterials,* 34 (24) (2013), pp. 5883–5890

[58]C. Wong, W. Lu, W. Chan, K. Cheung, K. Luk, D. Lu, *et al.* In vivo cancellous bone remodeling on a strontium-containing hydroxyapatite (sr-HA) bioactive cement. *J. Biomed. Mater. Res. A,* 68 (3) (2004), pp. 513–521

Corresponding author at: Department of Dental Biomaterials, Faculty of Dentistry, Tehran University of Medical Sciences, North Kargar Ave, Tehran 1439955991, Iran.